

Event-Based Secure Control of T–S Fuzzy-Based 5-DOF Active Semivehicle Suspension Systems Subject to DoS Attacks

Zhou Gu , Xiang Sun, Hak-Keung Lam , *Fellow, IEEE*, Dong Yue , *Fellow, IEEE*, and Xiangpeng Xie 

Abstract—This article investigates the problem of resilient secure control of cloud-aided 5-DOF active semivehicle suspension systems (SVSSs). A novel joint model considering both the event-triggered mechanism (ETM) and Denial of Service (DoS) attacks is established. Under such a model, during the active period of DoS attacks, periodic transmission attempt is made to ensure the control system can receive the control information at the earliest time; the ETM turns to be a conventional one when the DoS attack is in sleeping period. Meanwhile, the valid attack period is proposed to address the problem of the DoS attack ending within a sampling period, which is a challenging problem in modeling DoS attacks. Takagi–Sugeno (T–S) fuzzy model is used to characterize the uncertainties of sprung and unsprung mass of SVSSs. By converting the cloud-aided active SVSS into a fuzzy-based switched time-delay system, and using the method of piecewise Lyapunov function, sufficient conditions are derived to ensure the performances of active SVSSs subject to DoS attacks. Finally, the effectiveness of the proposed method is validated by a numerical example of active SVSSs subject to DoS attacks.

Index Terms—Active semivehicle suspension systems, event-triggered mechanism (ETM), Takagi–Sugeno (T–S) fuzzy model, valid DoS attack period.

I. INTRODUCTION

SUSPENSION systems play a crucial and important role in improving ride comfort and handling stability of vehicles driving on the uneven pavement [1]. Recent years have witnessed a widespread interest toward cloud-aided networked control of active suspension systems [2], [3]. Compared to traditional suspension systems, the road information of cloud-aided active suspension systems can be obtained in advance by using a vehicle Internet technology, and information among vehicles

can be exchanged more conveniently to achieve control decision, thereby improving the control performance [4]. Moreover, the use of cloud computing in the field of intelligent transportation can reduce a large number of complicated electronic devices and on-board storage in the vehicle [5]. However, signal transmission of cloud-aided active suspension systems via wireless network inevitably brings some new problems in control design, such as, network-induced delay [6], limited bandwidth [7], [8], and cyberattacks [9]–[11], etc. The suspension performance of vehicles with traditional control strategies cannot be ensured due to the existence of the network. Therefore, it is a big challenge for the control design of networked vehicle suspension systems, especially for the cloud-aided vehicle suspension systems with cyberattacks. For decades, there have been but not limited to this research conducted on these challenging issues, such as [12] and [13], and references therein.

Due to the reasons of communication, computation, and cost, the traditional suspension system with point-to-point communication has been upgraded to sample-based suspension systems [14]. Nowadays, the time-triggered communication scheme (TTCS) [15] is widely applied in practice. However, under the TTCS, not all the sampling data are necessary to improve the suspension performance. These redundant sampling data increase the burden on the network and the A/D converter. The event-triggered mechanism (ETM) is an alternation of TTCS since data packets are released only when the triggering condition is violated [16]–[18]. In [19], the ETM was applied to reduce the load of network communication in designing H_∞ controller for an active seat suspension. In order to solve the contradictory relationship between a better performance of the system and a lower data release rate, adaptive ETMs were proposed in [20] and [21], wherein the threshold of the adaptive ETM varies with the system state. In [22], an adaptive ETM-based fuzzy H_∞ control was developed for a quarter-suspension system to save the bandwidth and assure the performance. Besides, the memory-based ETM was another way to balance the system performance and the data release rate. In [23], the memory-based ETM was put forward to reduce the unnecessary transmission while improving the control performance.

It is noticed that the control signal of cloud-aided suspension systems is transmitted over the wireless network. Therefore, the problem of cybersecurity has to be considered in such a control framework. DoS attack, a common cyberattack mode, has received extensive concerns in the cyber-physical systems

Manuscript received January 18, 2021; revised March 30, 2021; accepted April 8, 2021. Date of publication April 14, 2021; date of current version June 2, 2022. This work was supported in part by the National Natural Science Foundation of China under Grant 62022044 and in part by the Jiangsu Natural Science Foundation for Distinguished Young Scholars under Grant BK20190039. (*Corresponding author: Zhou Gu.*)

Zhou Gu and Xiang Sun are with the College of Mechanical and Electronic Engineering, Nanjing Forestry University, Nanjing 210037, China (e-mail: gzh1808@163.com; sx032812@163.com).

Hak-Keung Lam is with the Department of Engineering, Kings College London, WC2R 2LS London, U.K. (e-mail: hak-keung.lam@kcl.ac.uk).

Dong Yue and Xiangpeng Xie are with the Institute of Advanced Technology, Nanjing University of Posts and Telecommunications, Nanjing 210023, China (e-mail: medongy@vip.163.com; xiexiangpeng1953@163.com).

Color versions of one or more figures in this article are available at <https://doi.org/10.1109/TFUZZ.2021.3073264>.

Digital Object Identifier 10.1109/TFUZZ.2021.3073264

(CPSs). The aim of DoS attack is to disrupt the access of control systems to communication network, thereby causing the deterioration of the system and bringing huge economic losses [24]. Hence, it is meaningful to consider the DoS attack in studying the cloud-aided suspension control systems. To the best of our knowledge, up to now, few results are involved in the control design of suspension systems under DoS attacks, which motivates our current study.

In recent years, considerable research efforts have been made on the secure control of networked control systems subject to DoS attacks. In [25], a model of periodic DoS jamming attacks inspired by energy constraints was studied for asymptotic stability of a continuous linear time-invariant system. The DoS attack model with the constrained frequency and duration was established for input-to-state stability of CPSs in [26]. Meanwhile, research on the resilient ETM-based control of CPSs against DoS attacks has motivated widespread interest (see [27]–[29]). However, in these existing models that consider both DoS attacks and ETMs, some scenarios that may happen in practice were not considered, such as DoS attack ending in a sampling interval. Therefore, much attention has focused on establishing a reasonable joint model considering both DoS attacks and ETM, which is another motivation for this article.

Takagi–Sugeno (T–S) model is a practical and effective method to describe the uncertainty of suspension systems, (see [30]–[32]). It is noted that the premise variables before and after the communication network of suspension systems are asynchronous. To deal with this problem, the control design of type 2 T–S fuzzy systems with mismatched membership functions was studied in [33]. However, few results are reported to study the problem of cloud-aided control of T–S fuzzy-based 5-DOF active SVSSs subject to DoS attacks.

Motivated by the above discussion, this article is concerned with T–S fuzzy H_∞ control for cloud-aided 5-DOF active SVSSs against DoS attacks. The main contributions of this article are summarized as follows.

- 1) A new DoS attack model is established, which considers the following two scenarios: a) the DoS attack ends within the sampling interval; and b) the start of a DoS attack and the end of the subsequent DoS attack occur in the same sampling interval. These two DoS attack intervals are integrated into one “*valid*” DoS attack (VDA) period.
- 2) A novel ETM model combining the VDA is put forward, under which periodic transmission attempts (PTAs), during the VDA period, continue until the valid DoS attack ends, and then the ETM generates a valid transmission event after the end of VDA. Based on this ETM and the VDA model, the suspension performance of cloud-aided active SVSSs can be ensured and the bandwidth of network can be saved as well.

The remainder of this article is organized as follows. Section II presents the system description and problem formulation. In Section III, the T–S fuzzy H_∞ control of the cloud-aided 5-DOF active SVSSs subject to DoS attacks is designed. An example of the 5-DOF suspension system is given in Section IV to show the effectiveness of the proposed method. Section V summarizes the article.

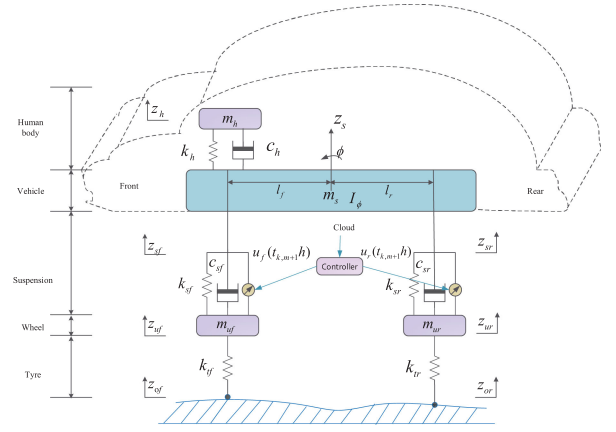


Fig. 1. Scheme diagram of active SVSSs.

II. PROBLEM FORMULATION

A. System Description and Performance Indicators

The schematic diagram of 5-DOF active SVSSs is shown in Fig. 1. Compared to the existing SVSSs with 4-DOFs in [34], the dynamic behavior of the chauffeur is considered in this model. In this article, the mass, movement, stiffness, and damping of the chauffeur are represented by m_h , z_h , k_h , and c_h , respectively. The other related physical quantities can be referred to [34].

Considering the pitch angle is small, we can get the following equations by using the linear approximation method:

$$\begin{cases} z_{sf}(t) = z_s(t) - l_f \phi(t) \\ z_{sr}(t) = z_s(t) + l_r \phi(t). \end{cases} \quad (1)$$

The vertical motion equation of the semivehicle body is modeled by

$$\begin{aligned} m_s \ddot{z}_s(t) = & -k_{sf}[z_{sf}(t) - z_{uf}(t)] + k_h[z_h(t) - z_{sf}(t)] \\ & -k_{sr}[z_{sr}(t) - z_{ur}(t)] - c_{sr}[\dot{z}_{sr}(t) - \dot{z}_{ur}(t)] \\ & -c_{sf}[\dot{z}_{sf}(t) - \dot{z}_{uf}(t)] + c_h[\dot{z}_h(t) - \dot{z}_{sf}(t)] \\ & + u_f(t) + u_r(t). \end{aligned} \quad (2)$$

Similarly, the vertical motion equations of the chauffeur, the front tyre and the rear tyre can be, respectively, described as

$$\begin{aligned} \ddot{z}_h(t) = & -\frac{k_h}{m_h}[z_h(t) - z_{sf}(t)] - \frac{c_h}{m_h}[\dot{z}_h(t) - \dot{z}_{sf}(t)] \\ \ddot{z}_{uf}(t) = & -\frac{1}{m_{uf}}u_f(t) + \frac{k_{sf}}{m_{uf}}[z_{sf}(t) - z_{uf}(t)] + \frac{c_{sf}}{m_{uf}} \\ & [\dot{z}_{sf}(t) - \dot{z}_{uf}(t)] - \frac{k_{tf}}{m_{uf}}[z_{uf}(t) - z_{of}(t)] \\ \ddot{z}_{ur}(t) = & -\frac{1}{m_{ur}}u_r(t) + \frac{k_{sr}}{m_{ur}}[z_{sr}(t) - z_{ur}(t)] + \frac{c_{sr}}{m_{ur}} \\ & [\dot{z}_{sr}(t) - \dot{z}_{ur}(t)] - \frac{k_{tr}}{m_{ur}}[z_{ur}(t) - z_{or}(t)] \end{aligned}$$

TABLE I
PERFORMANCE EVALUATION OF ACTIVE SVSSS

Indicator	Constraint condition
i) Ride comfort	$\ \ddot{z}_h(t) \ _2 + \ \ddot{\phi}(t) \ _2 \leq \gamma^2 \ \omega(t) \ _2$
ii) Suspension stroke	$ z_{sf}(t) - z_{uf}(t) \leq z_{smax}$ $ z_{sr}(t) - z_{ur}(t) \leq z_{rmax}$
iii) Road holding	$k_{tf}(z_{uf}(t) - z_{of}(t)) \leq G_f$ $k_{tr}(z_{ur}(t) - z_{or}(t)) \leq G_r$

and the pitching motion equation of the vehicle body can be established by

$$\begin{aligned}
I_\phi \ddot{\phi}(t) = & l_f k_{sf} [z_{sf}(t) - z_{uf}(t)] + l_f c_{sf} [\dot{z}_{sf}(t) \\
& - \dot{z}_{uf}(t)] - l_r k_{sr} [z_{sr}(t) - z_{ur}(t)] \\
& - l_r c_{sr} [\dot{z}_{sr}(t) - \dot{z}_{ur}(t)] - l_f k_h [z_h(t) \\
& - z_{sf}(t)] - l_f c_h [\dot{z}_h(t) - \dot{z}_{sf}(t)] \\
& - l_f u_f(t) + l_r u_r(t). \quad (3)
\end{aligned}$$

Similar to [22], the performance evaluation of active SVSSs in terms of ride comfort, suspension stroke, and road holding is shown in Table I.

In Table I, $\ddot{z}_h(t)$ and $\ddot{\phi}_h(t)$ in indicator i) are the body acceleration and pitch acceleration, which reflect the driver's comfort level; the indicator ii) and iii) consider the stroke of mechanical structure and vehicle driving safety, respectively. z_{smax} and z_{rmax} are the allowable stroke of mechanical structure of the front and rear suspension. G_f and G_r are the front and rear static load that can be calculated by

$$\begin{aligned}
G_f + G_r - (m_s + m_{uf} + m_{ur} + m_h)g &= 0 \\
G_r(l_f + l_r) - m_s g l_f - m_{uf} g(l_f + l_r) &= 0 \quad (4)
\end{aligned}$$

where g denotes gravitational acceleration.

For convenience of description, we define state vectors $x_1(t), \dots, x_{10}(t)$, and vectors $z_1(t)$ and $z_2(t)$ as follows:

$$\begin{aligned}
x_1(t) &= z_h(t) - z_{sf}(t), \quad x_2(t) = z_{sf}(t) - z_{uf}(t) \\
x_3(t) &= z_{uf}(t) - z_{of}(t), \quad x_4(t) = z_{sr}(t) - z_{ur}(t) \\
x_5(t) &= z_{ur}(t) - z_{or}(t), \quad x_6(t) = \dot{z}_h(t) \\
x_7(t) &= \dot{z}_{sf}(t), \quad x_8(t) = \dot{z}_{uf}(t), \quad x_9(t) = \dot{z}_{sr}(t) \\
x_{10}(t) &= \dot{z}_{ur}(t), \quad z_1(t) = \begin{bmatrix} \ddot{z}_h^T(t) & \ddot{\phi}^T(t) \end{bmatrix}^T \\
z_2(t) &= \begin{bmatrix} \underline{z}_f x_2^T(t) & \frac{k_{tf}}{G_f} x_3^T(t) & \underline{z}_r x_4^T(t) & \frac{k_{tr}}{G_r} x_5^T(t) \end{bmatrix}^T
\end{aligned}$$

where $\underline{z}_f = \frac{1}{z_{fmax}}$, $\underline{z}_r = \frac{1}{z_{rmax}}$, and the physical meanings of each state are listed in Table II.

To simplify the representation, we define

$$x(t) = [x_1^T(t) \ x_2^T(t) \ x_3^T(t) \ x_4^T(t) \ x_5^T(t) \ x_6^T(t) \ x_7^T(t)]^T$$

TABLE II
PHYSICAL MEANING OF THE STATES

State	Physical meaning
x_1	Deflection of human body
x_2	Suspension deflection of the front vehicle body
x_3	Tyre deflection of the front vehicle body
x_4	Suspension deflection of the rear vehicle body
x_5	Tyre deflection of the rear vehicle body
x_6	Velocity of the human body
x_7	Velocity of the front sprung mass
x_8	Velocity of the front unsprung mass
x_9	Velocity of the rear sprung mass
x_{10}	Velocity of the rear unsprung mass

$$x_8^T(t) \ x_9^T(t) \ x_{10}^T(t)]^T, \quad u(t) = [u_f^T(t) \ u_r^T(t)]^T$$

and

$$\omega(t) = [\dot{z}_{of}^T(t) \ \dot{z}_{or}^T(t)]^T$$

represent control input and the road disturbance, respectively. Then, the dynamics of active SVSSs in (1)–(3) can be written as

$$\begin{cases} \dot{x}(t) = Ax(t) + Bu(t) + D\omega(t) \\ z_1(t) = C_1 x(t) + D_1 u(t) \\ z_2(t) = C_2 x(t) \end{cases} \quad (5)$$

where

$$\begin{aligned}
A &= \begin{bmatrix} 0_{5 \times 5} & \tilde{A}_{12} \\ \tilde{A}_{21} & \tilde{A}_{22} \end{bmatrix}, \quad B = \begin{bmatrix} 0_{2 \times 6} & B_{12} \end{bmatrix}^T \\
C_1 &= \begin{bmatrix} C_{11} & C_{12} \end{bmatrix}^T, \quad C_2 = \begin{bmatrix} C_{21} & 0_{4 \times 5} \end{bmatrix}^T \\
D &= \begin{bmatrix} D_{11} & 0_{2 \times 5} \end{bmatrix}^T, \quad D_1 = \begin{bmatrix} 0 & 0 \\ -\frac{l_f}{I_\phi} & \frac{l_r}{I_\phi} \end{bmatrix} \\
\tilde{A}_{12} &= \begin{bmatrix} 1 & -1 & 0 & 0 & 0 \\ 0 & 1 & -1 & 0 & 0 \\ 0 & 0 & 1 & 0 & 0 \\ 0 & 0 & 0 & 1 & -1 \\ 0 & 0 & 0 & 0 & 1 \end{bmatrix} \\
\tilde{A}_{21} &= \begin{bmatrix} -\frac{k_h}{m_h} & 0 & 0 & 0 & 0 \\ k_h l_1 & -k_{sf} l_1 & 0 & -k_{sr} l_2 & 0 \\ 0 & \frac{k_{sf}}{m_{uf}} & -\frac{k_{tf}}{m_{uf}} & 0 & 0 \\ k_h l_2 & -k_{sf} l_2 & 0 & -k_{sr} l_3 & 0 \\ 0 & 0 & 0 & \frac{k_{sr}}{m_{ur}} & -\frac{k_{tr}}{m_{ur}} \end{bmatrix} \\
\tilde{A}_{22} &= \begin{bmatrix} -\frac{c_h}{m_h} & \frac{c_h}{m_h} & 0 & 0 & 0 \\ c_h l_1 & \hat{c} l_1 & c_{sf} l_1 & -c_{sr} l_2 & c_{sr} l_2 \\ 0 & \frac{c_{sf}}{m_{uf}} & -\frac{c_{sf}}{m_{uf}} & 0 & 0 \\ c_h l_2 & \hat{c} l_2 & c_{sf} l_2 & -c_{sr} l_3 & c_{sr} l_3 \\ 0 & 0 & 0 & \frac{c_{sr}}{m_{ur}} & -\frac{c_{sr}}{m_{ur}} \end{bmatrix}
\end{aligned}$$

$$\begin{aligned}
 B_{12} &= \begin{bmatrix} l_1 & -\frac{1}{m_{uf}} & l_2 & 0 \\ l_2 & 0 & l_3 & -\frac{1}{m_{ur}} \end{bmatrix}^T \\
 C_{11} &= \begin{bmatrix} -\frac{k_h}{m_h} & 0 & 0 & 0 & 0 \\ 0 & \frac{l_f k_{sf}}{I_\phi} & 0 & \frac{l_r k_{sr}}{I_\phi} & 0 \end{bmatrix} \\
 C_{12} &= \begin{bmatrix} -\frac{c_h}{m_h} & \frac{c_h}{m_h} & 0 & 0 & 0 \\ 0 & \frac{l_f c_{sf}}{I_\phi} & -\frac{l_f c_{sf}}{I_\phi} & -\frac{l_r c_{sr}}{I_\phi} & \frac{l_r c_{sr}}{I_\phi} \end{bmatrix} \\
 C_{21} &= \begin{bmatrix} 0 & \frac{1}{z_{fmax}} & 0 & 0 & 0 \\ 0 & 0 & \frac{k_{tf}}{G_f} & 0 & 0 \\ 0 & 0 & 0 & \frac{1}{z_{rmax}} & 0 \\ 0 & 0 & 0 & 0 & \frac{k_{tr}}{G_r} \end{bmatrix} \\
 D_{11} &= \begin{bmatrix} 0 & 0 & -1 & 0 & 0 \\ 0 & 0 & 0 & 0 & -1 \end{bmatrix}^T, \quad \hat{c} = -(c_h + c_{sf}) \\
 l_1 &= \frac{1}{m_s} + \frac{l_f^2}{I_\phi}, l_2 = \frac{1}{m_s} - \frac{l_f l_r}{I_\phi}, \quad l_3 = \frac{1}{m_s} + \frac{l_r^2}{I_\phi}.
 \end{aligned}$$

Considering that the uncertainty of the sprung mass ($m_s = m_s(t) \in [m_{smin}, m_{smax}]$), the front unsprung ($m_{uf} = m_{uf}(t) \in [m_{ufmin}, m_{ufmax}]$) and the rear unsprung ($m_{ur} = m_{ur}(t) \in [m_{urmin}, m_{urmax}]$), based on the T-S fuzzy modeling method, we choose $\frac{1}{m_s(t)}$ and $\frac{1}{m_u(t)}$ as premise variables and define the membership functions $F_{rs}(r \in \{1, 2\}, s \in \{1, 2\})$ of active SVSSs as follows:

$$\begin{aligned}
 F_{11}(\theta_1(t)) &= \frac{\frac{1}{m_s(t)} - \underline{m}_s}{\overline{m}_s - \underline{m}_s}, & F_{21}(\theta_1(t)) &= \frac{\overline{m}_s - \frac{1}{m_s(t)}}{\overline{m}_s - \underline{m}_s} \\
 F_{12}(\theta_2(t)) &= \frac{\frac{1}{m_u(t)} - \underline{m}_u}{\overline{m}_u - \underline{m}_u}, & F_{22}(\theta_2(t)) &= \frac{\overline{m}_u - \frac{1}{m_u(t)}}{\overline{m}_u - \underline{m}_u}
 \end{aligned}$$

where $\overline{m}_s = \frac{1}{m_{smin}}, \underline{m}_s = \frac{1}{m_{smax}}, \overline{m}_u = \frac{1}{m_{umin}}, \underline{m}_u = \frac{1}{m_{umax}}$.

Denote $\theta_1(t) \triangleq \frac{1}{m_s(t)}$ and $\theta_2(t) \triangleq \frac{1}{m_u(t)}$, respectively. It is obviously that $F_{1m}(\theta_m(t)) + F_{2m}(\theta_m(t)) = 1$ for $m \in \{1, 2\}$.

Then, the i th rule of T-S fuzzy-based active SVSSs in (5) can be expressed as follows.

Rule i : IF $\theta_1(t)$ is $F_{r1}, \dots, \theta_2(t)$ is F_{rs} , THEN

$$\begin{cases} \dot{x}(t) = A_i x(t) + B_i u(t) + D_i \omega(t) \\ z_1(t) = C_{1i} x(t) + D_{1i} u(t) \\ z_2(t) = C_{2i} x(t) \end{cases} \quad (6)$$

where the matrices $A_i, B_i, D_i, C_{1i}, C_{2i}$, and D_{1i} can be obtained by replacing $\frac{1}{m_s(t)}$ and $\frac{1}{m_u(t)}$ with \overline{m}_s (or \underline{m}_s) and \overline{m}_u (or \underline{m}_u) in matrices A, B, D, C_1, C_2 , and D_1 , respectively.

By utilizing center-average defuzzifier, singleton fuzzifier, and product inference, the overall active SVSS can be inferred as

$$\begin{cases} \dot{x}(t) = \sum_{i=1}^4 \varphi_i(\theta(t)) [A_i x(t) + B_i u(t) + D_i \omega(t)] \\ z_1(t) = \sum_{i=1}^4 \varphi_i(\theta(t)) [C_{1i} x(t) + D_{1i} u(t)] \\ z_2(t) = \sum_{i=1}^4 \varphi_i(\theta(t)) C_{2i} x(t) \end{cases} \quad (7)$$

where

$$\varphi_1(\theta(t)) = F_{11}(\theta_1(t)) \times F_{12}(\theta_2(t))$$

$$\varphi_2(\theta(t)) = F_{11}(\theta_1(t)) \times F_{22}(\theta_2(t))$$

$$\varphi_3(\theta(t)) = F_{21}(\theta_1(t)) \times F_{12}(\theta_2(t))$$

$$\varphi_4(\theta(t)) = F_{21}(\theta_1(t)) \times F_{22}(\theta_2(t)).$$

It is clear that $\sum_{i=1}^4 \varphi_i(\theta(t)) = 1$.

Remark 1: For simplicity, we assume $m_{uf}(t) = m_{ur}(t) = m_u(t)$, $m_{ufmin} = m_{urmin} = m_{umin}$, $m_{ufmax} = m_{urmax} = m_{umax}$ in this article.

B. Joint Model for the ETM and DoS Attacks

As discussed in Section I, the cloud-aided wireless network being a media of signal transmission for active SVSSs may generate some problems, such as the problem of limited bandwidth and cyberattacks, etc. In this article, a joint modeling approach is proposed to address these problems.

First, we consider the time sequence of the cloud-aided active SVSSs under the ETM. As shown in Fig. 2, the signal is sampled with a fixed sampling period h . Then, the sampling sequence can be expressed by the set $S_1 = \{0, h, 2h, \dots, kh\}, k \in \mathbb{N}^+$. Under the conventional ETM, only when transmission event is generated, the sampled data packet can be transmitted over the wireless network. The set of transmitted packets sequence is denoted by $S_2 = \{t_0 h, t_1 h, t_2 h, \dots, t_k h\}$. Obviously, $S_2 \subset S_1$.

Next, we consider the occurrence of DoS attacks on the wireless network. Under this scenario, the triggered packet cannot access the network terminal. Lack of active SVSS control input may lead to a degraded control performance or even instability.

Assume $\mathcal{D}(\bar{t}_1, \bar{t}_2)$ and $\mathcal{H}(\bar{t}_1, \bar{t}_2)$ are the time intervals of wireless network with and without DoS attacks in time interval $[\bar{t}_1, \bar{t}_2]$. They are defined as follows:

$$\mathcal{D}(\bar{t}_1, \bar{t}_2) = \bigcup_{n \in \mathbb{N}} D_n \cap [\bar{t}_1, \bar{t}_2] \quad (8)$$

$$\mathcal{H}(\bar{t}_1, \bar{t}_2) = [\bar{t}_1, \bar{t}_2] \setminus \mathcal{D}(\bar{t}_1, \bar{t}_2) \quad (9)$$

where D_n denotes the n th DoS attack interval with $D_n = [j_n, j_n + \tau_n)$ and $\tau_n \in \mathbb{R}_{\geq 0}$ is the duration of n th DoS attack. $\{j_n\}_{n \in \mathbb{N}}$ with $j_1 \geq 0$ denotes the set of start sequence of series DoS attacks.

Let us consider the following two scenarios about the DoS attack shown in Fig. 3, which is not involved in the existing literature.

1) The DoS attack ends within a sampling period, for example, the first DoS attack, in Fig. 3, ends at the instant $j_1 + \tau_1$, which is between the sampling instant 2 and 3 h. For this case, we regard the time interval $[\xi_1, \xi_1 + \nu_1)$ as a VDA period rather than $[j_1, j_1 + \tau_1)$ since the sampling packet cannot be released during the time interval $[j_1 + \tau_1, \xi_1 + \nu_1)$.

2) The end of the DoS attack and the start of next DoS attack are within the same sampling period, for example, both the end of the second DoS attack $j_2 + \tau_2$ and the start of the third DoS attack j_3 , in Fig. 3, are within the sampling period from 8 h to 9 h. Then, $[\xi_2, \xi_2 + \nu_2)$ is regarded as the second VDA period.

To better express VDAs, we define

$$\mathcal{F}_n = \{i | i \in \mathbb{N}, h_i = ih, h_i \in D_n\},$$

$$\lambda_n = h_s - j_n, s = \max_{i \in \mathcal{F}_n} i$$

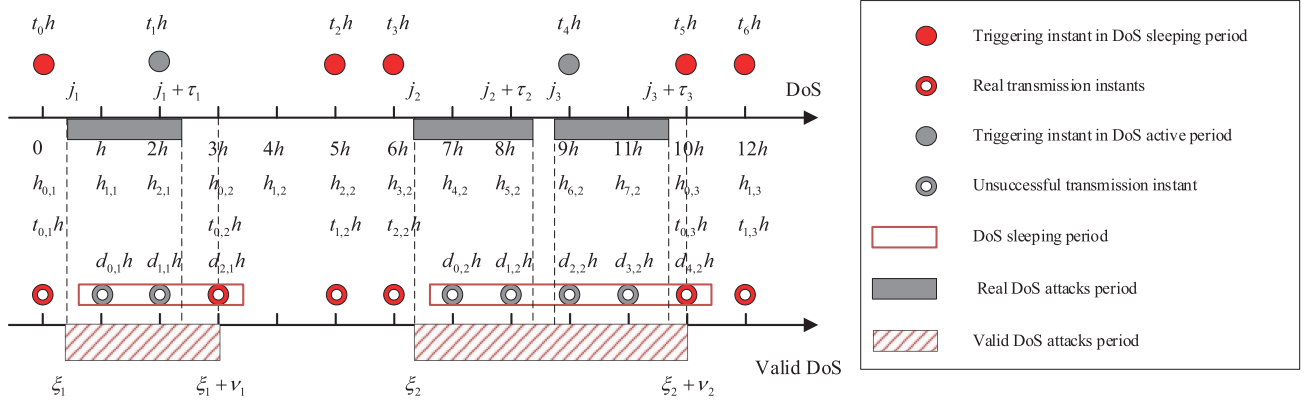


Fig. 2. Valid releasing sequence under the ETM and DoS attacks.

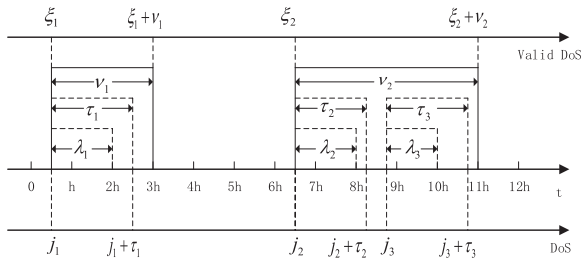


Fig. 3. Two cases of DoS attacks.

where \mathcal{F}_n is the set of the integer sequences, which consist of the i th sampling instants during DoS attack interval D_n ; for example, in Fig. 3, $\mathcal{F}_1 = \{1, 2\}$, $\mathcal{F}_2 = \{7, 8\}$.

For the second scenario above, one can find that j_3 in Fig. 3 is not a start of VDA any more. To deal with this problem, we redefine the start of VDA as ξ_m with $\xi_1 = j_1$ as follows:

$$\xi_{m+1} = \inf\{j_n \geq \xi_m | j_n > j_{n-1} + \lambda_{n-1} + h\}. \quad (10)$$

The duration of the m th VDA period can be expressed by

$$\nu_m = \sum_{\substack{n \in \mathbb{N} \\ \xi_m \leq j_n < \xi_{m+1}}} |\bar{D}_n \setminus \bar{D}_{n+1}| \quad (11)$$

where

$$\bar{D}_n = [j_n, j_n + \lambda_n + h). \quad (12)$$

Thus, the VDA period can be written by

$$\check{D}_m = [\xi_m, \xi_m + \nu_m). \quad (13)$$

Accordingly, $\check{\mathcal{H}}_m = [\xi_m + \nu_m, \xi_{m+1}) \cup [0, \xi_1)$ denotes the m th healthy period that there is no DoS attack within the interval $[\xi_m, \xi_{m+1}) \cup [0, \xi_1)$. For convenience, we assume $\xi_0 + \nu_0 = 0$. Then, $\check{\mathcal{H}}_m$ can be simplified as

$$\check{\mathcal{H}}_m = [\xi_m + \nu_m, \xi_{m+1}) \quad (14)$$

where $m \in \mathbb{N}_0$. It is clear that $\sum_{m=0}^{\infty} \check{D}_m \cup \check{\mathcal{H}}_m = [0, \infty)$.

To model the ETM that considers the occurrence of DoS attacks, we define

$$\begin{aligned} \psi(t) = e^T(t)W e(t) - \delta x^T(t_k h)W x(t_k h) \\ + \zeta(t_l h)\delta x^T(t_k h)W x(t_k h) \end{aligned} \quad (15)$$

where $e(t) = x(t_k h) - x(t_l h)$, $t_l h = t_k h + l h$, δ is a predefined constant and $\zeta(t_l h) \in \{0, 1\}$ is a detection signal, that is, when $t_l h \in \check{\mathcal{D}}_m$, the scalar $\zeta(t_l h)$ is set to be 1; otherwise, $t_l h \in \check{\mathcal{H}}_m$, the scalar $\zeta(t_l h)$ is set to be 0.

Based on the above definition, the next releasing instant can be expressed by

$$t_{k+1}h = t_k h + \max\{(l+1)h | \psi(t) < 0\}. \quad (16)$$

Remark 2: If the detection signal $\zeta(t_l h)$ in (15) equals to 1, then $\psi(t) > 0$ is always held. Consequently, triggering events will be generated with a sampling period h during VDA period. We call this behavior as ‘‘PTA.’’ Although the controller can not receive packets from the network during DoS attack, the controller can receive the latest packet from the plant after the DoS attack ends; once the system is under healthy with $\zeta(t_l h) = 0$, the ETM turns to be a traditional ETM as in [16].

Due to the PTA, the packet at the end of DoS attack will also be enabled to transmit over the network. Therefore, we need to redefine (13) and (14) as

$$\begin{aligned} \bar{D}_m &= [\xi_m, \xi_m + \nu_m] \\ \bar{\mathcal{H}}_m &= (\xi_m + \nu_m, \xi_{m+1}). \end{aligned} \quad (17)$$

Then, considering the ETM model in (16) and DoS attacks model in (17) together, we can rewrite the next real transmitting instant $t_{k,m+1}h$ as

$$\begin{aligned} t_{k,m+1}h \in \{t_l h \text{ satisfying (16)} | t_l h \in \bar{\mathcal{H}}_m\} \\ \cup \{\xi_m + \nu_m\} \end{aligned} \quad (18)$$

where $m, l \in \mathbb{N}_0$, $t_{0,m+1}h = \xi_m + \nu_m$.

Remark 3: In [27], the start and the end of DoS attacks are assumed to occur at sampling instant, which is seriously strict, and it is hard to meet this assumption in practice. To address this

problem, we propose a new definition of the PTA during DoS attacks and the VDA period in this article.

C. Closed-Loop Control of Active SVSSs

In this section, we will construct the closed-loop control of active SVSSs considering both the DoS attack and the ETM.

Before developing the control law for the active SVSS, we first give the following definitions:

$$q(m) = \sup\{q \in \mathbb{N}_0 | h_{q,m+1} < \xi_{m+1} + \nu_{m+1}\}$$

$$p(m) = \inf\{q \in \mathbb{N}_0 | h_{q,m+1} \geq \xi_{m+1}\}$$

$$s(m) = \sup\{s \in \mathbb{N}_0 | d_{s,m+1}h \leq \xi_{m+1}\}$$

$$k(m) = \sup\{k \in \mathbb{N}_0 | t_{k,m+1}h < \xi_{m+1}\}.$$

Remark 4: In the above definition, $q(m)$ denotes the number of sampling periods from the m th end of DoS attack to the $(m+1)$ th end of DoS attack, i.e., $q(m) = (\xi_{m+1} + \nu_{m+1} - \xi_m - \nu_m)/h - 1$, $h_{0,m+1}, h_{1,m+1}, \dots, h_{q(m),m+1}$ are sampling instants during m th DoS attack period. $h_{p(m),m+1}$ and $d_{s(m),m+1}h$ denote the first sampling instant and the last sampling instant in active period of DoS attacks, respectively; and $t_{k(m),h}$ denotes the last releasing instant in sleeping period of DoS attacks. In Fig. 3, taking $m = 1$ as an example, from the above definition, one can obtain: $q(1) = 7; p(1) = 4; s(1) = 4$; and $k(1) = 2$.

Define $\mathcal{G}_{s,m} = [d_{s,m+1}h, d_{s+1,m+1}h)$ for $s \in \{0, 1, \dots, s(m)\}$. Then, one can know that the VDA period is $\sum_{s=0}^{s(m)} \mathcal{G}_{s,m} \cap \bar{\mathcal{D}}_m$.

Define the set $\mathcal{V}_{k,m} \triangleq \mathcal{R}_{k,m} \cap \bar{\mathcal{H}}_m$ and the set $\bar{\mathcal{V}}_{s,m} \triangleq \mathcal{G}_{s,m} \cap \bar{\mathcal{D}}_m$. Then, under DoS attacks and the ETM, we develop the fuzzy controller for the active SVSS as follows.

Controller Rule j: If $\theta_1(t_{k,m+1}h)$ is $F_{r1}, \dots, \theta_s(t_{k,m+1}h)$ is F_{rs} , THEN

$$u(t) = \begin{cases} K_j x(t_{k,m+1}h), & t \in \mathcal{V}_{k,m} \\ 0, & t \in \bar{\mathcal{V}}_{s,m} \end{cases} \quad (19)$$

where $K_j (j = 1, 2, 3, 4)$ is the control gain to be designed, and $\mathcal{R}_{k,m} = [t_{k,m+1}h, t_{k+1,m+1}h)$ for $k \in \{0, 1, \dots, k(m)\}$.

Combining (7) and (19), we can get the the following switched T-S fuzzy-based closed-loop active SVSSs with two modes as follows:

$$\begin{cases} \dot{x}(t) = \begin{cases} \chi(t), & t \in \mathcal{V}_{k,m} \\ \sum_{i=1}^4 \varphi_i(\theta(t)) [A_i x(t) + D_i \omega(t)], & t \in \bar{\mathcal{V}}_{s,m} \end{cases} \\ z_1(t) = \begin{cases} \chi_1(t), & t \in \mathcal{V}_{k,m} \\ \sum_{i=1}^4 \varphi_i(\theta(t)) C_{1i} x(t), & t \in \bar{\mathcal{V}}_{s,m} \end{cases} \\ z_2(t) = \sum_{i=1}^4 \varphi_i(\theta(t)) C_{2i} x(t) \end{cases} \quad (20)$$

where

$$\begin{aligned} \chi(t) &= \sum_{i=1}^4 \sum_{j=1}^4 \varphi_i(\theta(t)) \varphi_j(\theta(t_{k,m+1}h)) [A_i x(t) \\ &\quad + B_i K_j x(t_{k,m+1}h) + D_i \omega(t)] \end{aligned}$$

$$\begin{aligned} \chi_1(t) &= \sum_{i=1}^4 \sum_{j=1}^4 \varphi_i(\theta(t)) \varphi_j(\theta(t_{k,m+1}h)) [C_{1i} x(t) \\ &\quad + D_{1i} K_j x(t_{k,m+1}h)]. \end{aligned}$$

In the following, for brevity, we use φ_i and φ_j^k to replace $\varphi_i(\theta(t))$ and $\varphi_j(\theta(t_{k,m+1}h))$, respectively. In addition, similar to [29], it is assumed that $\varphi_j^k - \rho_j \varphi_j \geq 0$.

Meanwhile, based on the above discussion, $\psi(t)$ in (15) can be rewritten as

$$\psi(t) = \begin{cases} \psi_h(t), & t \in \mathcal{V}_{k,m} \\ \tilde{e}_{s,m+1}^T(t) W \tilde{e}_{s,m+1}(t), & t \in \bar{\mathcal{V}}_{s,m} \end{cases} \quad (21)$$

where $\psi_h(t) = e_{k,m+1}^T(t) W e_{k,m+1}(t) - \delta x^T(t_{k,m+1}h) W x(t_{k,m+1}h)$ with $e_{k,m+1}(t) = x(t_{k,m+1}h) - x(t_{k,m+1}h + lh)$ and $\tilde{e}_{s,m+1}(t) = x(d_{s,m+1}h) - x(d_{s,m+1}h + lh)$.

Accordingly, $d_{s+1,m+1}h = d_{s,m+1}h + h$, and $t_{k+1,m+1}h = t_{k,m+1}h + l_M h + h$ with $l_M = \max\{l | \psi(t) < 0, t \in \mathcal{V}_{k,m}\}$.

Defining $\eta(t) = t - t_{k,m+1}h - lh$ for $t \in \mathcal{V}_{k,m}$ yields that

$$x(t_{k,m+1}h) = e_{k,m+1}(t) + x(t - \eta(t)). \quad (22)$$

By combining (20)–(22), we have

$$\begin{cases} \dot{x}(t) = \begin{cases} \hat{\chi}(t), & t \in \mathcal{V}_{k,m} \\ \sum_{i=1}^4 \varphi_i [A_i x(t) + D_i \omega(t)], & t \in \bar{\mathcal{V}}_{s,m} \end{cases} \\ z_1(t) = \begin{cases} \hat{\chi}_1(t), & t \in \mathcal{V}_{k,m} \\ \sum_{i=1}^4 \varphi_i C_{1i} x(t), & t \in \bar{\mathcal{V}}_{s,m} \end{cases} \\ z_2(t) = \sum_{i=1}^4 \varphi_i C_{2i} x(t) \end{cases} \quad (23)$$

where

$$\begin{aligned} \hat{\chi}(t) &= \sum_{i=1}^4 \sum_{j=1}^4 \varphi_i \varphi_j^k [A_i x(t) + B_i K_j x(t - \eta(t)) \\ &\quad + B_i K_j e_{k,m+1}(t) + D_i \omega(t)] \\ \hat{\chi}_1(t) &= \sum_{i=1}^4 \sum_{j=1}^4 \varphi_i \varphi_j^k [C_{1i} x(t) + D_{1i} K_j x(t - \eta(t)) \\ &\quad + D_{1i} K_j e_{k,m+1}(t)]. \end{aligned}$$

For convenience of analysis, we define $\mathcal{I}_{g,m} = [t_{g,m}, t_{3-g,m+g-1})$, where

$$t_{g,m} = \begin{cases} \xi_m + \nu_m, & g = 1 \\ \xi_{m+1}, & g = 2 \end{cases}. \quad (24)$$

Then, the active SVSS can be reformulated as the following switched system:

$$\begin{cases} \dot{x}(t) = \tilde{\chi}(t), & t \in [t_{g,m}, t_{3-g,m+g-1}) \\ z_1(t) = \tilde{\chi}_1(t), & t \in [t_{g,m}, t_{3-g,m+g-1}) \\ z_2(t) = \sum_{i=1}^4 \varphi_i C_{2i} x(t) \end{cases} \quad (25)$$

where

$$\begin{aligned}\tilde{\chi}(t) &= \sum_{i=1}^4 \sum_{j=1}^4 \varphi_i \varphi_j^k [A_{ij}^g x(t) + B_{ij}^g x(t - \eta(t)) \\ &\quad + B_{ij}^g e_{k,m+1}(t) + D_{ij}^g \omega(t)] \\ \tilde{\chi}_1(t) &= \sum_{i=1}^4 \sum_{j=1}^4 \varphi_i \varphi_j^k [C_{1i}^g x(t) + D_{1ij}^g x(t - \eta(t)) \\ &\quad + D_{1ij}^g e_{k,m+1}(t)]\end{aligned}$$

with $A_{ij}^g = A_i, B_{ij}^1 = B_i K_j, B_{ij}^2 = 0, C_{1i}^g = C_{1i}, D_{ij}^g = D_i, D_{1ij}^1 = D_{1i} K_j, D_{1ij}^2 = 0$.

Remark 5: The switched system in (25) has two modes—DoS sleeping mode with $g = 1$ and DoS active mode with $g = 2$.

The main objective of this article is to design the resilient secure controller and the ETM such that the active SVSS in (25) is exponential stable with H_∞ attenuation lever γ .

III. MAIN RESULTS

In this section, we aim to analyze the stability of event-triggered active SVSSs subject to DoS attacks, and then present the criterion of controller design for the active SVSS. Before doing these, we first give the following definition and assumptions.

Definition 1: The switched system (25) is exponentially stable with an H_∞ norm bound γ if the following hold:

- 1) when $\omega(t) = 0$, the system (25) is exponentially stable;
- 2) under zero initial conditions, for a scalar $\gamma > 0$ and any nonzero $\omega(t) \in \mathcal{L}_2[0, \infty)$ satisfies $\sum_{t=0}^{\infty} \|z_1(t)\|_2 \leq \sum_{t=0}^{\infty} \gamma^2 \|\omega(t)\|_2$.

Similar to [26], the VDA satisfies the following assumptions.

Assumption 1: (DoS frequency): For any $0 \leq \bar{t}_1 < \bar{t}_2$, there exists $\varsigma_1 \in \mathbb{R}_{\geq 0}$ and $\eta_D \in \mathbb{R}_{> 0}$ such that

$$m(\bar{t}_1, \bar{t}_2) \leq \varsigma_1 + \frac{(\bar{t}_2 - \bar{t}_1)}{\eta_D}. \quad (26)$$

Assumption 2: (DoS duration): For any $0 \leq \bar{t}_1 < \bar{t}_2$, there exists $\varsigma_2 \in \mathbb{R}_{\geq 0}$ and $\eta_T \in \mathbb{R}_{> 1}$ such that

$$|\mathcal{D}(\bar{t}_1, \bar{t}_2)| \leq \varsigma_2 + \frac{(\bar{t}_2 - \bar{t}_1)}{\eta_T}. \quad (27)$$

Remark 6: $m(\bar{t}_1, \bar{t}_2)$ in (26) and $\mathcal{D}(\bar{t}_1, \bar{t}_2)$ in (27) mean the number of valid DoS and union of valid DoS intervals in the intervals $[\bar{t}_1, \bar{t}_2]$, respectively. $\frac{1}{\eta_D}$ and $\frac{1}{\eta_T}$ represent the upper bound on average frequency and duration of valid DoS per unit time, respectively.

Theorem 1: For given positive scalars $h, \alpha_g, \mu_g > 1, \delta \in (0, 1)$ and $\varsigma_g \in \mathbb{R}_{\geq 0}, \eta_D, \eta_T \in \{\eta | \eta \in \mathbb{R}_{\geq 0}, \bar{\tau} > 0\}$, and matrices K_j with $j \in \{1, 2, 3, 4\}$, the system (25) is exponentially stable with H_∞ norm bound γ and the decay rate $\bar{\tau}$, if there exist symmetric matrices $P_g > 0, Q_g > 0, R_g > 0, W > 0, H > 0$ and M_{gi} such that

$$\mathcal{M}_{ijg} < 0 \quad (28)$$

$$\mathcal{M}_{iig} + M_{gi} < 0 \quad (29)$$

$$\mathcal{M}_{ijg} + \mathcal{M}_{jig} + M_{gi} + M_{gj} < 0, (i < j) \quad (30)$$

$$P_1 \leq \mu_2 P_2 \quad (31)$$

$$P_2 \leq e^{2(\alpha_1 + \alpha_2)h} \mu_1 P_1 \quad (32)$$

$$Q_g \leq \mu_{3-g} Q_{3-g} \quad (33)$$

$$R_g \leq \mu_{3-g} R_{3-g} \quad (34)$$

$$\begin{bmatrix} -I & * \\ \sqrt{\nu} \{C_{2i}\}_s^T & -P_g \end{bmatrix} < 0, (s = 1, 2) \quad (35)$$

$$\mathcal{R} = \begin{bmatrix} \hat{R}_1 & * \\ H^T & \hat{R}_1 \end{bmatrix} > 0 \quad (36)$$

$$\mathcal{N} = \begin{bmatrix} \hat{R}_2 & * \\ N^T & \hat{R}_2 \end{bmatrix} > 0 \quad (37)$$

for $g = 1, 2$, where

$$\mathcal{M}_{ijg} = \rho_j (\Phi_{ij}^g - M_{gi}), \quad \mathcal{W}_1 = b_1 \mathcal{T}_1^T \mathcal{R} \mathcal{T}_1$$

$$\Phi_{ij}^g = \begin{bmatrix} \Pi_{11}^{gij} + \mathcal{W}_g & * \\ \Pi_{21}^{gij} & \Pi_{22}^{gij} \end{bmatrix}$$

$$\mathcal{W}_2 = b_2 \mathcal{T}_2^T \mathcal{N} \mathcal{T}_2, \quad \mathcal{T}_g = \begin{bmatrix} T_{g1}^T & T_{g2}^T & T_{g3}^T & T_{g4}^T \end{bmatrix}^T$$

$$T_{11} = [I \quad -I \quad 0 \quad 0 \quad 0 \quad 0 \quad 0]$$

$$T_{12} = [I \quad I \quad 0 \quad 0 \quad -2I \quad 0 \quad 0]$$

$$T_{13} = [0 \quad I \quad -I \quad 0 \quad 0 \quad 0 \quad 0]$$

$$T_{14} = [0 \quad I \quad I \quad 0 \quad 0 \quad -2I \quad 0]$$

$$T_{21} = [I \quad -I \quad 0 \quad 0 \quad 0 \quad 0 \quad 0]$$

$$T_{22} = [I \quad I \quad 0 \quad -2I \quad 0 \quad 0 \quad 0]$$

$$T_{23} = [0 \quad I \quad -I \quad 0 \quad 0 \quad 0 \quad 0]$$

$$T_{24} = [0 \quad I \quad I \quad 0 \quad -2I \quad 0 \quad 0]$$

$$\Pi_{11}^{1ij} = \begin{bmatrix} \Psi_{11}^{1ij} & * \\ \Psi_{21}^{1ij} & \Psi_{22}^{1ij} \end{bmatrix}, \quad \Pi_{11}^{2ij} = \begin{bmatrix} \Psi_{11}^{2ij} & * \\ \Psi_{21}^{2ij} & \Psi_{22}^{2ij} \end{bmatrix}$$

$$\Pi_{21}^{1ij} = \begin{bmatrix} c_1 A_i & c_1 B_i K_j & 0 & c_1 B_i K_j & 0 & 0 & c_1 D_i \\ C_{1i} & D_{1i} K_j & 0 & D_{1i} K_j & 0 & 0 & 0 \end{bmatrix}$$

$$\Pi_{21}^{2ij} = \begin{bmatrix} c_2 A_i & 0 & 0 & 0 & 0 & c_2 D_i \\ C_{1i} & 0 & 0 & 0 & 0 & 0 \end{bmatrix}$$

$$\Pi_{22}^{gij} = \text{diag}\{-R_g^{-1}, -I\}, \quad \Psi_{11}^{1ij} = \begin{bmatrix} \Xi_{11}^{1ij} & * & * \\ \Xi_{21}^{1ij} & \Xi_{22}^{1ij} & * \\ 0 & 0 & \Xi_{33}^{1ij} \end{bmatrix}$$

$$\Psi_{11}^{2ij} = \begin{bmatrix} \Xi_{11}^{2ij} & * & * \\ 0 & 0 & * \\ 0 & 0 & \Xi_{33}^{2ij} \end{bmatrix}, \quad \Psi_{21}^{1ij} = \begin{bmatrix} \Xi_{21}^{1ij} & \delta W & 0 \\ 0 & 0 & 0 \\ 0 & 0 & 0 \\ D_i^T P_1 & 0 & 0 \end{bmatrix}$$

$$\Psi_{21}^{2ij} = \begin{bmatrix} 0 & 0 & 0 \\ 0 & 0 & 0 \\ D_i^T P_2 & 0 & 0 \end{bmatrix}, \Psi_{22}^{2ij} = \begin{bmatrix} 0 & * & * \\ 0 & 0 & * \\ 0 & 0 & -\gamma^2 I \end{bmatrix}$$

$$\Psi_{22}^{1ij} = \begin{bmatrix} (\delta - 1)W & * & * & * \\ 0 & 0 & * & * \\ 0 & 0 & 0 & * \\ 0 & 0 & 0 & -\gamma^2 I \end{bmatrix},$$

$$\Xi_{11}^{gij} = P_g A_i + A_i^T P_g + (-1)^{g+1} 2\alpha_g P_g + Q_g,$$

$$\Xi_{21}^{1ij} = K_j^T B_i^T P_1, \Xi_{22}^{1ij} = \delta W, \Xi_{33}^{gij} = a_g Q_g$$

$$\hat{R}_g = \begin{bmatrix} R_g & 0 \\ 0 & 3R_g \end{bmatrix}, H = \begin{bmatrix} H_1 & * \\ H_2 & H_3 \end{bmatrix}$$

$$a_1 = -e^{-2\alpha_1 h}, a_2 = -e^{-2\alpha_2 h}, b_1 = \frac{a_1}{h},$$

$$b_2 = -\frac{1}{h}, c_1 = c_2 = \sqrt{h}, N = \begin{bmatrix} N_1 & * \\ N_2 & N_3 \end{bmatrix}.$$

$$\bar{t} = \alpha_1 - \frac{1}{\eta T}(\alpha_1 + \alpha_2) - \frac{1}{\eta D}((\alpha_1 + \alpha_2)h + \ln \sqrt{\mu_1 \mu_2}).$$

Proof: For the switched system (25), we choose the following piecewise Lyapunov functional:

$$V_g(t) = x^T(t)P_g x(t) + \int_{t-h}^t x^T(s)\varrho_g(s,t)Q_g x(s)ds + \int_{-h}^0 \int_{t+\theta}^t \dot{x}^T(s)\varrho_g(s,t)R_g \dot{x}(s)dsd\theta \quad (38)$$

where $\varrho_g(s,t) = e^{2(-1)^g \alpha_g (t-s)}$.

For $g = 1$, taking derivative on $V_g(t)$, one can obtain

$$\begin{aligned} \dot{V}_1(t) \leq & -2\alpha_1 V_1(t) + x^T(t)2\alpha_1 P_1 x(t) \\ & + \dot{x}^T(t)2P_1 x(t) + x^T(t)Q_1 x(t) \\ & + a_1 x^T(t-h)Q_1 x(t-h) \\ & + a_1 \int_{t-h}^t \dot{x}^T(s)R_1 \dot{x}(s)ds + h\dot{x}^T(t)R_1 \dot{x}(t). \end{aligned} \quad (39)$$

Define $\Gamma_1(t) = [x^T(t) \ x^T(t-\eta(t)) \ x^T(t-h) \ e^T(t) \frac{1}{\eta(t)} \int_{t-\eta(t)}^t x^T(s)ds \frac{1}{h-\eta(t)} \int_{t-h}^{t-\eta(t)} x^T(s)ds \ \omega^T(t)]^T$.

Applying Wirtinger inequality [35] yields that

$$\begin{aligned} \int_{t-\eta(t)}^t \dot{x}^T(s)R_1 \dot{x}(s)ds & \geq \frac{1}{\eta(t)} \hat{\Omega}_1^T(t) \hat{R}_1 \hat{\Omega}_1(t) \\ \int_{t-h}^{t-\eta(t)} \dot{x}^T(s)R_1 \dot{x}(s)ds & \geq \frac{1}{h-\eta(t)} \hat{\Omega}_2^T(t) \hat{R}_1 \hat{\Omega}_2(t) \end{aligned} \quad (40)$$

where

$$\hat{\Omega}_1(t) = \begin{bmatrix} T_{11} \\ T_{12} \end{bmatrix} \Gamma_1(t), \hat{\Omega}_2(t) = \begin{bmatrix} T_{13} \\ T_{14} \end{bmatrix} \Gamma_1(t).$$

From (40) and the approach in [36], it can be derived that

$$\begin{aligned} & a_1 \int_{t-h}^t \dot{x}^T(s)R_1 \dot{x}(s)ds \\ & \leq b_1 \begin{bmatrix} \hat{\Omega}_1(t) \\ \hat{\Omega}_2(t) \end{bmatrix}^T \begin{bmatrix} \frac{h}{\eta(t)} \hat{R}_1 & 0 \\ 0 & \frac{h}{h-\eta(t)} \hat{R}_1 \end{bmatrix} \begin{bmatrix} \hat{\Omega}_1(t) \\ \hat{\Omega}_2(t) \end{bmatrix} \\ & \leq b_1 \begin{bmatrix} \hat{\Omega}_1(t) \\ \hat{\Omega}_2(t) \end{bmatrix}^T \mathcal{R} \begin{bmatrix} \hat{\Omega}_1(t) \\ \hat{\Omega}_2(t) \end{bmatrix}. \end{aligned} \quad (41)$$

Notice that

$$h\dot{x}^T(t)R_1 \dot{x}(t) \leq h \sum_{i=1}^4 \sum_{j=1}^4 \varphi_i \varphi_j^k \Gamma_1^T(t) \mathcal{A}^T R_1 \mathcal{A} \Gamma_1(t) \quad (42)$$

where $\mathcal{A} = [A_i \ B_i K_j \ 0 \ B_i K_j \ 0 \ 0 \ D_i]$.

Combining (21), (39), (41), (42), and applying the Schur complement, we have

$$\begin{aligned} & \dot{V}_1(t) + z_1^T(t)z_1(t) - \gamma^2 \omega^T(t)\omega(t) \\ & \leq -2\alpha_1 V_1(t) + \sum_{i=1}^4 \sum_{j=1}^4 \varphi_i \varphi_j^k \Gamma_1^T(t) \Phi_{ij}^1 \Gamma_1(t). \end{aligned} \quad (43)$$

Using a similar method in [29] to deal with the problem of membership function mismatch, one can obtain

$$\begin{aligned} & \sum_{i=1}^4 \sum_{j=1}^4 \varphi_i \varphi_j^k \Gamma_1^T(t) \Phi_{ij}^1 \Gamma_1(t) \\ & \leq \sum_{i=1}^4 \sum_{j=1}^4 \varphi_i \varphi_j \Gamma_1^T(t) [\rho_i(\Phi_{ii}^1 - M_{1i}) + M_{1i}] \Gamma_1(t) \\ & \quad + \sum_{i=1}^4 \sum_{i < j} \varphi_i \varphi_j \Gamma_1^T(t) [\rho_j(\Phi_{ij}^1 - M_{1i}) \\ & \quad + \rho_i(\Phi_{ji}^1 - M_{1j}) + M_{1i} + M_{1j}] \Gamma_1(t). \end{aligned}$$

Then, it can be known that (28)–(30) are sufficient conditions to ensure

$$\dot{V}_1(t) + 2\alpha_1 V_1(t) + z_1^T(t)z_1(t) - \gamma^2 \omega^T(t)\omega(t) < 0. \quad (44)$$

For $g = 2$, we define $\Gamma_2(t) = [x^T(t), x^T(t-\eta(t)), x^T(t-h), \frac{1}{\eta(t)} \int_{t-\eta(t)}^t x^T(s)ds, \frac{1}{h-\eta(t)} \int_{t-h}^{t-\eta(t)} x^T(s)ds, \omega(t)]^T$.

Similarly, from (28)–(30), it yields that

$$\dot{V}_2(t) - 2\alpha_2 V_2(t) + z_1^T(t)z_1(t) - \gamma^2 \omega^T(t)\omega(t) < 0. \quad (45)$$

For $\omega(t) = 0$, we can obtain

$$\begin{cases} V_1(t) \leq e^{-2\alpha_1(t-t_{1,m})} V_1(t_{1,m}), & t \in \mathcal{I}_{1,m} \\ V_2(t) \leq e^{2\alpha_2(t-t_{2,m})} V_2(t_{2,m}), & t \in \mathcal{I}_{2,m} \end{cases} \quad (46)$$

from Theorem 1.

In the light of (31)–(34), one has

$$\begin{cases} V_1(t_{1,m}) \leq \mu_2 V_2(t_{1,m}^-) \\ V_2(t_{2,m}) \leq e^{2(\alpha_1 + \alpha_2)h} \mu_1 V_1(t_{2,m}^-). \end{cases} \quad (47)$$

From (46) and (47), it follows that

$$\begin{aligned} V(t) &\leq \mu_2 e^{-2\alpha_1(t-t_{1,m})} V_2(t_{1,m}^-) \\ &\leq \mu_2 e^{-2\alpha_1(t-t_{1,m})+2\alpha_2(t_{1,m}-t_{2,m-1})} V_2(t_{2,m-1}) \\ &\vdots \\ &\leq (\mu_1 \mu_2)^m e^{q_1(t)+2(\alpha_1+\alpha_2)hm} V(t_{1,0}) \end{aligned} \quad (48)$$

for $t \in [t_{1,m}, t_{2,m})$, where $q_1(t) = -2\alpha_1[(t-t_{1,m}) + (t_{2,m-1}-t_{1,m-1}) + \dots + (t_{2,0}-t_{1,0})] + 2\alpha_2[(t_{1,m}-t_{2,m-1}) + (t_{1,m-1}-t_{2,m-2}) + \dots + (t_{1,1}-t_{2,0})]$ with $t_{1,0} = 0$.

Define $\iota(t) = q_1(t) + 2(\alpha_1 + \alpha_2)hm + m \ln(\mu_1 \mu_2)$. From (26) and (27), it has

$$\begin{aligned} \iota(t) &\leq -2\alpha_1(t - \frac{t}{\eta_T}) + 2\alpha_2 \frac{t}{\eta_D} \\ &\quad + 2(\alpha_1 + \alpha_2)h \frac{t}{\eta_D} + \frac{t}{\eta_D} \ln(\mu_1 \mu_2) \\ &= -2\bar{\iota}t. \end{aligned} \quad (49)$$

where $\bar{\iota} > 0$ is defined in Theorem 1.

Combining (48) and (49) yields that

$$V(t) \leq e^{-2\bar{\iota}t} V(0). \quad (50)$$

Similarly, for $t \in [t_{2,m}, t_{1,m+1})$, one can obtain

$$\begin{aligned} V(t) &\leq \mu_1^{m+1} \mu_2^m e^{q_2(t)+2(\alpha_1+\alpha_2)h(m+1)} V(0) \\ &\leq e^{-2\bar{\iota}t+\ln\mu_1+2(\alpha_1+\alpha_2)h} V(0) \end{aligned} \quad (51)$$

with $q_2(t) = -2\alpha_1[(t_{2,m}-t_{1,m}) + (t_{2,m-1}-t_{1,m-1}) + \dots + (t_{2,0}-t_{1,0})] + 2\alpha_2[(t-t_{2,m}) + (t_{1,m}-t_{2,m-1}) + (t_{1,m-1}-t_{2,m-2}) + \dots + (t_{1,1}-t_{2,0})]$.

Notice that

$$\mathcal{M} \triangleq e^{\ln\mu_1+2(\alpha_1+\alpha_2)h} > 1 \quad (52)$$

for $\mu_g > 1, \alpha_g > 0$ with $g = 1, 2$.

Then, considering (50) and (51) together, we have

$$V(t) \leq \mathcal{M} e^{-2\bar{\iota}t} V(0). \quad (53)$$

From (38), it follows that

$$V(t) \geq \epsilon_1 \|x(t)\|^2, V_1(0) \leq \epsilon_2 \|v_0\|_h^2 \quad (54)$$

where $\epsilon_1 = \min\{\lambda_{\min}(P_g)\}$, $\epsilon_2 = \max\{\lambda_{\max}(P_g) + h\lambda_{\max}(Q_g) + (h^2/2)\lambda_{\max}(R_g)\}$, $v(t)$ is the supplemented initial condition of the state $x(t)$, $v(0) = v_0$, $\|v_0\|_h = \sup_{-h \leq \hat{v} \leq 0} \{|\dot{v}(t+\hat{v})|, |v(t+\hat{v})|\}$.

Combining (53) and (54) yields that

$$\|x(t)\| > \sqrt{\frac{\mathcal{M}\epsilon_2}{\epsilon_1}} e^{-\bar{\iota}t} \|v_0\|_h \quad (55)$$

which implies that the system (25) is exponentially stable with the decay rate $\bar{\iota}$.

For $\omega(t) \neq 0$, integrating (44) and (45) for $t \in \mathcal{I}_{g,m}$ follows that

$$\sum_{i=0}^m \int_{t_{1,m}}^t [\dot{V}_g(t) - (-1)^g 2\alpha_g V_g(t) + z_1^T(t) z_1(t)$$

$$- \gamma^2 \omega^T(t) \omega(t)] dt \leq 0. \quad (56)$$

Letting $m \rightarrow \infty$ follows that

$$\int_0^\infty z_1^T(t) z_1(t) dt \leq \gamma^2 \int_0^\infty \omega^T(t) \omega(t) dt. \quad (57)$$

From Definition 1, one can obtain that the switched system (25) is exponentially stable with an H_∞ norm bound γ .

In addition, from (39) and (56), it follows that

$$x^T(t) P_g x(t) \leq \nu \quad (58)$$

where $\nu = \inf_{t>0} \{V(0) + \int_0^t [z_1^T(t) z_1(t) - \gamma^2 \omega^T(t) \omega(t)] dt\}$.

To ensure the indicator ii) and iii) in Table I, it requires that

$$|\{z_2(t)\}_s| \leq I \quad (s = 1, 2) \quad (59)$$

where $\{z_2(t)\}_s$ denotes the s th line of $z_2(t)$.

From (58), one can obtain

$$\begin{aligned} &\sum_{i=1}^4 \mu_i^t [x^T(t) \{C_{2i}\}_s^T \{C_{2i}\}_s x(t)] \\ &= \sum_{i=1}^4 \mu_i^t [x^T(t) P_g^{\frac{1}{2}} P_g^{-\frac{1}{2}} \{C_{2i}\}_s^T \{C_{2i}\}_s P_g^{-\frac{1}{2}} P_g^{\frac{1}{2}} x(t)] \\ &\leq \lambda_{\max} \left\{ \sum_{i=1}^4 \mu_i^t [\nu P_g^{-\frac{1}{2}} \{C_{2i}\}_s^T \{C_{2i}\}_s P_g^{-\frac{1}{2}}] \right\} \end{aligned}$$

where $\lambda_{\max}\{\cdot\}$ represents the maximal eigenvalue, and $\{C_{2i}\}_s$ denotes the s th line of C_{2i} .

Using Schur complement to (35) yields that

$$\nu P_g^{-\frac{1}{2}} \{C_{2i}\}_s^T \{C_{2i}\}_s P_g^{-\frac{1}{2}} \leq I.$$

Then, we have

$$\begin{aligned} &\max_{t>0} |\{z_2(t)\}_s|^2 \\ &\leq \max_{t>0} \left\| \sum_{i=1}^2 \mu_i^t [x^T(t) \{C_{2i}\}_s^T \{C_{2i}\}_s x(t)] \right\|_2 \\ &\leq I \end{aligned} \quad (60)$$

which means (59) can be held, i.e., the indicator ii) and iii) in Table I can be guaranteed. This completes the proof. \square

Theorem 2: For given positive scalars $h, \alpha_g, \epsilon_g, \mu_g > 1$, $\delta \in [0, 1]$ and $\varsigma_g \in \mathbb{R}_{\geq 0}$, $\eta_D, \eta_T \in \{\eta | \eta \in \mathbb{R}_{\geq 0}, \bar{\iota} > 0\}$, the system (25) is exponentially stable with H_∞ norm bound γ and decay rate $\bar{\iota}$, if there exist positive symmetric matrices $X_g, \tilde{Q}_g, \tilde{R}_g, \tilde{W}, \tilde{H}$, and matrix $\tilde{M}_{gi}^T = \tilde{M}_{gi}$ such that

$$\mathcal{N}_{ijg} < 0 \quad (61)$$

$$\mathcal{N}_{iig} + \tilde{M}_{gi} < 0 \quad (62)$$

$$\mathcal{N}_{ijg} + \mathcal{N}_{jig} + \tilde{M}_{gi} + \tilde{M}_{gj} < 0 \quad (i < j) \quad (63)$$

$$\begin{bmatrix} -\mu_2 X_2 & * \\ X_2 & -X_1 \end{bmatrix} \leq 0 \quad (64)$$

$$\begin{bmatrix} -\mu_1 e^{2(\alpha_1+\alpha_2)h} X_1 & * \\ X_1 & -X_2 \end{bmatrix} \leq 0 \quad (65)$$

$$\begin{bmatrix} -\mu_{3-g}\tilde{Q}_{3-g} & * \\ X_{3-g} & -2\varepsilon_g X_g + \varepsilon_g^2 \tilde{Q}_g \end{bmatrix} \leq 0 \quad (66)$$

$$\begin{bmatrix} -\mu_{3-g}\tilde{R}_{3-g} & * \\ X_{3-g} & -2\varepsilon_g X_g + \varepsilon_g^2 \tilde{R}_g \end{bmatrix} \leq 0 \quad (67)$$

$$\begin{bmatrix} -I & * \\ \sqrt{\nu}X_g\{C_{2i}\}_s^T & -X_g \end{bmatrix} < 0, (s = 1, 2) \quad (68)$$

$$\tilde{\mathcal{R}} = \begin{bmatrix} \tilde{R}_1 & * \\ \tilde{H}^T & \tilde{R}_1 \end{bmatrix} > 0 \quad (69)$$

$$\tilde{\mathcal{N}} = \begin{bmatrix} \tilde{R}_2 & * \\ \tilde{N}^T & \tilde{R}_2 \end{bmatrix} > 0 \quad (70)$$

for $g = 1, 2$, where

$$\mathcal{N}_{ijg} = \rho_j(\tilde{\Phi}_{ij}^g - \tilde{M}_{gi}), \tilde{\mathcal{W}}_1 = b_1 \mathcal{T}_1^T \tilde{\mathcal{R}} \mathcal{T}_1$$

$$\tilde{\Phi}_{ij}^g = \begin{bmatrix} \tilde{\Pi}_{11}^{gij} + \tilde{\mathcal{W}}_g & * \\ \tilde{\Pi}_{21}^{gij} & \tilde{\Pi}_{22}^{gij} \end{bmatrix}, \mathcal{W}_2 = b_2 \mathcal{T}_2^T \tilde{\mathcal{N}} \mathcal{T}_2$$

$$\tilde{\Pi}_{11}^{1ij} = \begin{bmatrix} \tilde{\Psi}_{11}^{1ij} & * \\ \tilde{\Psi}_{21}^{1ij} & \tilde{\Psi}_{22}^{1ij} \end{bmatrix}, \tilde{\Pi}_{11}^{2ij} = \begin{bmatrix} \tilde{\Psi}_{11}^{2ij} & * \\ \tilde{\Psi}_{21}^{2ij} & \tilde{\Psi}_{22}^{2ij} \end{bmatrix}$$

$$\tilde{\Pi}_{21}^{1ij} = \begin{bmatrix} c_1 A_i X_1 & c_1 B_i Y_j & 0 & c_1 B_i Y_j & 0 & 0 & c_1 D_i \\ C_{1i} X_1 & D_{1i} Y_j & 0 & D_{1i} Y_j & 0 & 0 & 0 \end{bmatrix}$$

$$\tilde{\Pi}_{21}^{2ij} = \begin{bmatrix} c_2 A_i X_2 & 0 & 0 & 0 & 0 & c_2 D_i \\ C_{1i} X_2 & 0 & 0 & 0 & 0 & 0 \end{bmatrix}$$

$$\tilde{\Pi}_{22}^{gij} = \text{diag}\{-2\varepsilon_g X_g + \varepsilon_g^2 \tilde{R}_g, -I\}$$

$$\tilde{\Psi}_{11}^{1ij} = \begin{bmatrix} \tilde{\Xi}_{11}^{1ij} & * & * \\ \tilde{\Xi}_{21}^{1ij} & \tilde{\Xi}_{22}^{1ij} & * \\ 0 & 0 & \tilde{\Xi}_{33}^{1ij} \end{bmatrix}, \tilde{\Psi}_{21}^{1ij} = \begin{bmatrix} \tilde{\Xi}_{21}^{1ij} & \delta \tilde{W} & 0 \\ 0 & 0 & 0 \\ 0 & 0 & 0 \\ D_i^T & 0 & 0 \end{bmatrix}$$

$$\tilde{\Psi}_{22}^{1ij} = \begin{bmatrix} (\delta - 1)\tilde{W} & * & * & * \\ 0 & 0 & * & * \\ 0 & 0 & 0 & * \\ 0 & 0 & 0 & -\gamma^2 I \end{bmatrix}$$

$$\tilde{\Psi}_{11}^{2ij} = \begin{bmatrix} \tilde{\Xi}_{11}^{2ij} & * & * \\ 0 & 0 & * \\ 0 & 0 & \tilde{\Xi}_{33}^{2ij} \end{bmatrix}, \tilde{\mathcal{N}} = \begin{bmatrix} \tilde{N}_1 & * \\ \tilde{N}_2 & \tilde{N}_3 \end{bmatrix}$$

$$\tilde{\Psi}_{21}^{2ij} = \begin{bmatrix} 0 & 0 & 0 \\ 0 & 0 & 0 \\ D_i^T & 0 & 0 \end{bmatrix}, \tilde{\Psi}_{22}^{2ij} = \begin{bmatrix} 0 & * & * \\ 0 & 0 & * \\ 0 & 0 & -\gamma^2 I \end{bmatrix}$$

$$\tilde{\Xi}_{11}^{gij} = A_i X_g + X_g A_i^T + (-1)^{g+1} 2\alpha_g X_g + \tilde{Q}_g$$

$$\tilde{\Xi}_{21}^{1ij} = Y_j^T B_i^T, \tilde{\Xi}_{22}^{1ij} = \delta \tilde{W}, \tilde{\Xi}_{33}^{gij} = a_g \tilde{Q}_g$$

$$\tilde{R}_g = \begin{bmatrix} \tilde{R}_g & 0 \\ 0 & 3\tilde{R}_g \end{bmatrix}, \tilde{H} = \begin{bmatrix} \tilde{H}_1 & * \\ \tilde{H}_2 & \tilde{H}_3 \end{bmatrix}.$$

TABLE III
NOMINAL PARAMETERS OF THE 5-DOF ACTIVE SVSS

quantity	value	quantity	value
$m_h(kg)$	43.4	$c_h(Ns/m)$	1485
$c_{sf}(Ns/m)$	1000	$c_{sr}(Ns/m)$	1000
$k_{sf}(N/m)$	18000	$k_{sr}(N/m)$	18000
$k_{tf}(N/m)$	200000	$k_{tr}(N/m)$	200000
$l_f(m)$	1.3	$l_r(m)$	1.3
$I_\phi(kgm^2)$	1222	$k_h(N/m)$	44

and the other parameters are defined in Theorem 1. Moreover, the proposed resilient secure controller gain and the event-triggered weighted matrix can be calculated by $K_j = Y_j X_1^{-1}$ and $W = X_1^{-1} \tilde{W} X_1^{-1}$, respectively.

Proof: Define

$$\mathcal{I} = \text{diag}\{\underbrace{I, \dots, I}_6\}, \mathcal{X}_1 = \text{diag}\{\underbrace{X_1, \dots, X_1}_6\},$$

$$J_1 = \text{diag}\{\mathcal{I}, I, P_1, I\}, \mathcal{X}_2 = \text{diag}\{\underbrace{X_2, \dots, X_2}_5\},$$

$$J_2 = \text{diag}\{\mathcal{I}, P_2, I\}, U_1 = \text{diag}\{\mathcal{X}_1, I, X_1, I\},$$

$$U_2 = \text{diag}\{\mathcal{X}_2, I, X_2, I\}, \tilde{W} = X_1 W X_1,$$

$$\tilde{H} = \begin{bmatrix} \tilde{H}_1 & * \\ \tilde{H}_2 & \tilde{H}_3 \end{bmatrix}, \tilde{H}_1 = X_1 H_1 X_1, \tilde{H}_2 = X_1 H_2 X_1,$$

$$\tilde{H}_3 = X_1 H_3 X_1, \tilde{N} = \begin{bmatrix} \tilde{N}_1 & * \\ \tilde{N}_2 & \tilde{N}_3 \end{bmatrix}, \tilde{N}_1 = X_2 N_1 X_2,$$

$$\tilde{N}_2 = X_2 N_2 X_2, \tilde{N}_3 = X_2 N_3 X_2, \tilde{Q}_g = X_g Q_g X_g,$$

$$\tilde{R}_g = X_g R_g X_g, \tilde{M}_{gi} = U_g M_{gi} U_g, \tilde{M}_{gj} = U_g M_{gj} U_g,$$

$$X_g = P_g^{-1}, K_j = Y_j X_1^{-1}.$$

Notice that $(\varepsilon_g R_g - P_g) R_g^{-1} (\varepsilon_g R_g - P_g) \geq 0$, we have $-P_g R_g^{-1} P_g \leq -2\varepsilon_g P_g + \varepsilon_g^2 R_g$.

Then, pre- and postmultiplying (28) with $U_g J_g$ and $J_g U_g$, it can be concluded that (61) is a sufficient condition to ensure (28). Similarly, we can achieve (62) and (63) can ensure (29) and (30), respectively.

Applying the Schur complement to (31) and pre- and postmultiplying $\text{diag}\{X_2, X_1\}$, respectively, it yields that (64) is equivalent to (31). Using a similar method, one can obtain (65)–(67) hold from (31)–(34). Pre- and postmultiplying (28) with $\text{diag}\{I, X_g\}$ knows that (35) is a sufficient condition to ensure (68) holds. This completes the proof. \square

Remark 7: Theorems 1 and 2 are derived based on the methods of VDA and PTA. Under this strategy, the suspension systems can update the control signal at the earliest time after DoS attacks so as to get satisfied suspension performance.

IV. SIMULATION

In this section, an example of the 5-DOF SVSS in Fig. 1 is presented to show the effectiveness of our proposed method. The sprung mass m_s varies from 621 to 759 kg, the front and rear unsprung mass vary from 39.6 to 40.4 kg and the other parameters of the 5-DOF active SVSS are listed in Table III.

TABLE IV
NPR, NDS, AND DRR IN DIFFERENT TIME INTERVALS

time (s)	0-0.75	0.75-1.00	1.00-2.76	2.76-3.00	3.00-5.05	5.05-5.35	5.35-6.00
	(valid DoS period)		(valid DoS period)		(valid DoS period)		
NDS (TTCS)	75	25	176	24	205	30	65
NPR (ETM)	31	1	53	1	59	1	18
DRR	41.33%	4.00%	30.11%	4.16%	28.78%	3.33%	27.69%

The bump road profile is considered as follows [5]:

$$z_{of}(t) = \begin{cases} \frac{A}{2}(1 - \cos(\frac{2\pi V_0}{l}t)), & 0 \leq t \leq \frac{l}{V_0} \\ 0, & t > \frac{l}{V_0} \end{cases}$$

$$z_{or}(t) = \begin{cases} 0, & 0 \leq t < \tau_l \\ \frac{A}{2}(1 - \cos(\frac{2\pi V_0}{l}(t - \tau_l))), & \tau_l \leq t \leq \bar{\tau}_l \\ 0, & t > \bar{\tau}_l \end{cases} \quad (71)$$

where A and l refer to the height and length of the bump, respectively. Here, we select $A = 0.1$ m, $l = 5$ m, $V_0 = 45$ km/h, $\bar{\tau}_l = \frac{l}{V_0} + \tau_l$ with $\tau_l = \frac{lf+lr}{V_0}$.

Suppose $h = 0.01$ s, $\gamma = 29.16$, $\delta = 0.04$, $\alpha_1 = 0.01$, $\alpha_2 = 0.005$, $\mu_1 = \mu_2 = 1.01$, $\rho_1 = 0.95$, $\rho_2 = 0.8$, $\rho_3 = 0.7$, $\rho_4 = 0.85$, $\varepsilon_1 = \varepsilon_2 = 4.5$, $\nu = 0.64$, $z_{fmax} = z_{rmax} = 0.01$ m, $\eta_D = 2$, $\eta_T = 5$, $\varsigma_1 = \varsigma_2 = 0$. From Assumptions 1, 2, and scalars $\eta_D, \eta_T, \varsigma_1, \varsigma_2$, the DoS attacks in simulation should satisfy the conditions that the DoS frequency $m(0, 6)$ in (26) is no more than 3 s within 6 s and the DoS duration $\mathcal{D}(0, 6)$ in (27) does not exceed 1.2 s within 6 s.

By using Theorem 2, we can get the fuzzy controller gains K_1 as

$$K_1 = 10^4 \times \begin{bmatrix} K_{11} & K_{12} & K_{13} \end{bmatrix},$$

with

$$K_{11} = \begin{bmatrix} 0.0044 & 0.0038 & 1.2437 \\ -0.0009 & -0.4483 & -0.3469 \end{bmatrix}$$

$$K_{12} = \begin{bmatrix} 0.0683 & 0.2247 & 0.1490 \\ -0.3480 & 0.6280 & -0.0293 \end{bmatrix}$$

$$K_{13} = \begin{bmatrix} -0.4940 & 0.0308 & -0.0771 & -0.0064 \\ -0.0767 & -0.0061 & -0.1052 & 0.0750 \end{bmatrix}$$

and the other parameters, such as K_i with $i = 2, 3, 4$ and event-triggered weighted matrix W are not listed here due to the limited space.

Fig. 4 shows the responses of the main indicators of suspension systems listed in Table I, wherein the black solid lines depict the responses by using our purposed method. Compared to the passive SVSS whose responses are plotted in red dash line, one can see the cloud-aided 5-DOF SVSS with our proposed method can result in better suspension performances, that is to say, under DoS attacks, our proposed method can ensure the cloud-aided suspension systems to a certain lever against the bump road profile. Fig. 4(a) shows that the ride comfort of the chauffeur is greatly improved.

Fig. 5 depicts the real data transmission instants ($t_{k,m}h$) and releasing intervals. Yellow rectangular regions indicate the VDA

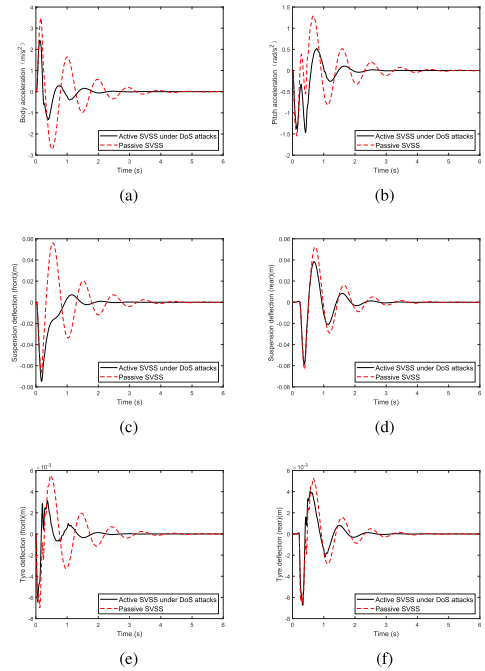


Fig. 4. Responses of the active SVSS under DoS attacks and the passive SVSS.

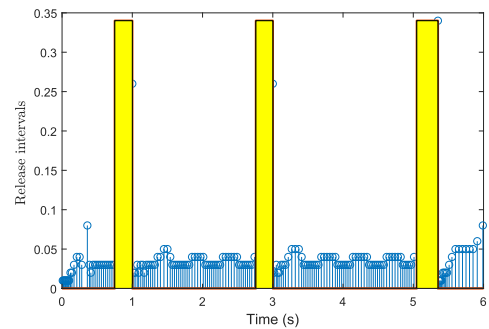


Fig. 5. Release intervals of the active SVSS under DoS attacks.

period and PTAs are made during this period. To better describe the effect of our proposed joint ETM, statistical result about the number of packet releasing (NPR), the number of data sampling (NDS), and data releasing rate (DRR) in different time intervals are listed in Table IV, where DRR is defined by $DRR = \frac{NPR}{NDS}$. From Table IV, one can know that the number of valid sampling data (excluding DoS attack period) is 521 within 6 s, while the real number of transmission data is 164, i.e., the average DRR within 6 s is 27.33%, which implies that the network burden can be greatly reduced by using our method. Besides, Table IV shows that DRR during the period 0–0.75 s is greater than other periods and the DRR gradually decreases as the system tends to be stable.

V. CONCLUSION

This article had been dealt with the problem of resilient secure control for cloud-aided 5-DOF active SVSSs based on the proposed joint model considering both DoS attacks and the ETM. T-S fuzzy model had been used to describe the uncertainty of suspension systems. To save the network bandwidth and ensure the secure control networked suspension system, a joint model of the DoS attacks and ETM had been proposed. Under such a model, PTAs were made during the active period of DoS attacks so that the controller could receive the information of the active SVSS at the earliest time; the VDA period was defined to address the scenario of the end of DoS attack within a sampling period. Resilient secure control strategy was designed by converting the hybrid closed-loop SVSS into switched time-delay systems based on the proposed joint model. Finally, expected performances of active SVSS subject to DoS attacks had been obtained by an example of real active SVSSs, which demonstrated the efficiency of the proposed approach. In the future, we will focus on modeling new ETMs, such as memory ETM and adaptive ETM, to address networked suspension control systems.

REFERENCES

- [1] H. Li, H. Liu, H. Gao, and P. Shi, "Reliable fuzzy control for active suspension systems with actuator delay and fault," *IEEE Trans. Fuzzy Syst.*, vol. 20, no. 2, pp. 342–357, Apr. 2011.
- [2] A. Mihály, Á. Kisari, P. Gáspár, and B. Németh, "Adaptive semi-active suspension design considering cloud-based road information," *IFAC-Papers On Line*, vol. 52, no. 5, pp. 249–254, 2019.
- [3] C. Yang, J. Xia, J. H. Park, H. Shen, and J. Wang, "Sliding mode control for uncertain active vehicle suspension systems: An event-triggered h_∞ control scheme," *Nonlinear Dyn.*, vol. 103, pp. 3209–3221, Mar. 2021.
- [4] L. Liu and X. Li, "Event-triggered tracking control for active seat suspension systems with time-varying full-state constraints," *IEEE Trans. Syst. Man Cybern. Syst.*, to be published, doi: [10.1109/TSMC.2020.3003368](https://doi.org/10.1109/TSMC.2020.3003368).
- [5] H. Zhang, X. Zheng, H. Yan, C. Peng, Z. Wang, and Q. Chen, "Co-design of event-triggered and distributed H_∞ filtering for active semi-vehicle suspension systems," *IEEE/ASME Trans. Mechatronics*, vol. 22, no. 2, pp. 1047–1058, Apr. 2017.
- [6] X. Yin, L. Zhang, Y. Zhu, C. Wang, and Z. Li, "Robust control of networked systems with variable communication capabilities and application to a semi-active suspension system," *IEEE/ASME Trans. Mechatronics*, vol. 21, no. 4, pp. 2097–2107, Aug. 2016.
- [7] Y. Liu, B. Guo, J. H. Park, and S. Lee, "Event-based reliable dissipative filtering for T-S fuzzy systems with asynchronous constraints," *IEEE Trans. Fuzzy Syst.*, vol. 26, no. 4, pp. 2089–2098, Aug. 2018.
- [8] D. Zhang, Q.-L. Han, and X.-M. Zhang, "Network-based modeling and proportional-integral control for direct-drive-wheel systems in wireless network environments," *IEEE Trans. Cybern.*, vol. 50, no. 6, pp. 2462–2474, Jun. 2020.
- [9] A.-Y. Lu and G.-H. Yang, "Distributed consensus control for multi-agent systems under denial-of-service," *Inf. Sci.*, vol. 439, pp. 95–107, May 2018.
- [10] X. Jiang, X. Mu, and Z. Hu, "Decentralized adaptive fuzzy tracking control for a class of nonlinear uncertain interconnected systems with multiple faults and DoS attack," *IEEE Trans. Fuzzy Syst.*, to be published, doi: [10.1109/TFUZZ.2020.3013700](https://doi.org/10.1109/TFUZZ.2020.3013700).
- [11] X. Ge, Q.-L. Han, M. Zhong, and X.-M. Zhang, "Distributed Krein space-based attack detection over sensor networks under deception attacks," *Automatica*, vol. 109, Nov. 2020, Art. no. 108557.
- [12] H. Li, H. Liu, H. Gao, and P. Shi, "Reliable fuzzy control for active suspension systems with actuator delay and fault," *IEEE Trans. Fuzzy Syst.*, vol. 20, no. 2, pp. 342–357, Apr. 2012.
- [13] X. Zheng, H. Zhang, H. Yan, F. Yang, and L. Vlacic, "Active full-vehicle suspension control via cloud-aided adaptive backstepping approach," *IEEE Trans. Cybern.*, vol. 50, no. 7, pp. 3113–3124, Jul. 2020.
- [14] T. H. Lee, J. H. Park, "New methods of fuzzy sampled-data control for stabilization of chaotic systems," *IEEE Trans. Syst. Man Cybern. Syst.*, vol. 48, no. 12, pp. 2026–2034, Dec. 2017.
- [15] Z. Ju, H. Zhang, and Y. Tan, "Distributed deception attack detection in platoon-based connected vehicle systems," *IEEE Trans. Veh. Technol.*, vol. 69, no. 5, pp. 4609–4620, May 2020.
- [16] D. Yue, E. Tian, and Q.-L. Han, "A delay system method for designing event-triggered controllers of networked control systems," *IEEE Trans. Autom. Control*, vol. 58, no. 2, pp. 475–481, Feb. 2013.
- [17] B.-L. Zhang, Q.-L. Han, and X.-M. Zhang, "Event-triggered H_∞ reliable control for offshore structures in network environments," *J. Sound Vib.*, vol. 368, pp. 1–21, Apr. 2016.
- [18] D. Wang, Z. Wang, Z. Wang, and W. Wang, "Design of hybrid event-triggered containment controllers for homogeneous and heterogeneous multiagent systems," *IEEE Trans. Cybern.*, to be published, doi: [10.1109/TCYB.2020.3007500](https://doi.org/10.1109/TCYB.2020.3007500).
- [19] W. Li, H. Du, and D. Ning, "Event-triggered H_∞ control for active seat suspension systems based on relaxed conditions for stability," *Mech. Syst. Signal Process.*, vol. 149, Feb. 2021, Art. no. 107210.
- [20] Z. Gu, P. Shi, D. Yue, and Z. Ding, "Decentralized adaptive event-triggered H_∞ filtering for a class of networked nonlinear interconnected systems," *IEEE Trans. Cybern.*, vol. 49, no. 5, pp. 1570–1579, May 2019.
- [21] Z. Fei, S. Shi, C. K. Ahn, and M. Basin, "Finite-time control for switched T-S fuzzy systems via dynamic event-triggered mechanism," *IEEE Trans. Fuzzy Syst.*, to be published, doi: [10.1109/TFUZZ.2020.3029292](https://doi.org/10.1109/TFUZZ.2020.3029292).
- [22] H. Li, Z. Zhang, H. Yan, and X. Xie, "Adaptive event-triggered fuzzy control for uncertain active suspension systems," *IEEE Trans. Cybern.*, vol. 49, no. 12, pp. 4388–4397, Dec. 2019.
- [23] E. Tian and C. Peng, "Memory-based event-triggering H_∞ load frequency control for power systems under deception attacks," *IEEE Trans. Cybern.*, vol. 50, no. 11, pp. 4610–4618, Nov. 2020.
- [24] D. Ding, Q.-L. Han, X. Ge, and J. Wang, "Secure state estimation and control of cyber-physical systems: A survey," *IEEE Trans. Syst. Man Cybern. Syst.*, vol. 51, no. 1, pp. 176–190, Jan. 2021.
- [25] H. S. Foroush and S. Martinez, "On event-triggered control of linear systems under periodic denial-of-service jamming attacks," in *Proc. 51st Annu. Conf. Decis. Control*, Dec. 2012, pp. 2551–2556.
- [26] C. De Persis and P. Tesi, "Input-to-state stabilizing control under denial-of-service," *IEEE Trans. Autom. Control*, vol. 60, no. 11, pp. 2930–2944, Nov. 2015.
- [27] S. Hu, D. Yue, X. Xie, X. Chen, and X. Yin, "Resilient event-triggered controller synthesis of networked control systems under periodic DoS jamming attacks," *IEEE Trans. Cybern.*, vol. 49, no. 12, pp. 4271–4281, Dec. 2019.
- [28] S. Li, C. K. Ahn, and Z. Xiang, "Decentralized sampled-data control for cyber-physical systems subject to DoS attacks," *IEEE Syst. J.*, to be published, doi: [10.1109/JSYST.2020.3019939](https://doi.org/10.1109/JSYST.2020.3019939).
- [29] J. Liu, T. Yin, J. Cao, D. Yue, and H. R. Karimi, "Security control for T-S fuzzy systems with adaptive event-triggered mechanism and multiple cyber-attacks," *IEEE Trans. Syst. Man Cybern. Syst.*, to be published, doi: [10.1109/TSMC.2019.2963143](https://doi.org/10.1109/TSMC.2019.2963143).
- [30] J. Zhang, F. Ding, B. Zhang, C. Jiang, H. Du, and B. Li, "An effective projection-based nonlinear adaptive control strategy for heavy vehicle suspension with hysteretic leaf spring," *Nonlinear Dyn.*, vol. 100, no. 1, pp. 451–473, Mar. 2020.
- [31] X. Shao, F. Naghdy, Du, and B. Li, "Reliable fuzzy H_∞ control for active suspension of in-wheel motor driven electric vehicles with dynamic damping," *Mech. Syst. Signal Process.*, vol. 87, pp. 365–383, Mar. 2017.
- [32] J. Lian and S. Li, "Fuzzy control of uncertain positive Markov jump fuzzy systems with input constraint," *IEEE Trans. Cybern.*, vol. 51, no. 4, pp. 2032–2041, Apr. 2021.
- [33] H. K. Lam, "A review on stability analysis of continuous-time fuzzy-model-based control systems: From membership-function-independent to membership-function-dependent analysis," *Eng. Appl. Artif. Intell.*, vol. 67, pp. 390–408, Jan. 2018.
- [34] H. Li, X. Jing, H. K. Lam, and S. Peng, "Fuzzy sampled-data control for uncertain vehicle suspension systems," *IEEE Trans. Cybern.*, vol. 44, no. 7, pp. 1111–1126, Jul. 2014.
- [35] A. Seuret and F. Gouaisbaut, "Wirtinger-based integral inequality: Application to time-delay systems," *Automatica*, vol. 49, no. 9, pp. 2860–2866, Sep. 2013.
- [36] A. Seuret, F. Gouaisbaut, and E. Fridman, "Stability of systems with fast-varying delay using improved Wirtinger's inequality," in *Proc. 52nd IEEE Conf. Decis. Control*, 2013, pp. 946–951.